CORE
Metadata, citation and similar papers at core.ac.uk
Provided by Elsevier - Publisher Connector

Available online at www.sciencedirect.com
ScienceDirect
Biochimica et Biophysica Acta 1757 (2006) 1162–1170
BIOCHIMICA ET BIOPHYSICA ACTA
BBA
www.elsevier.com/locate/bbabio

Review

ATP synthase: Subunit–subunit interactions in the stator stalk

Joachim Weber *

Texas Tech University, Department of Chemistry and Biochemistry, Lubbock, TX 79409-1061, USA

Received 20 February 2006; received in revised form 20 March 2006; accepted 5 April 2006
Available online 19 April 2006

Abstract

In ATP synthase, proton translocation through the F_o subcomplex and ATP synthesis/hydrolysis in the F_1 subcomplex are coupled by subunit rotation. The static, non-rotating portions of F_1 and F_o are attached to each other via the peripheral "stator stalk", which has to withstand elastic strain during subunit rotation. In *Escherichia coli*, the stator stalk consists of subunits $b_2\delta$; in other organisms, it has three or four different subunits. Recent advances in this area include affinity measurements between individual components of the stator stalk as well as a detailed analysis of the interaction between subunit δ (or its mitochondrial counterpart, the oligomycin-sensitivity conferring protein, OSCP) and F_1. The current status of our knowledge of the structure of the stator stalk and of the interactions between its subunits will be discussed in this review.
© 2006 Elsevier B.V. All rights reserved.

Keywords: ATP synthase; F_1-ATPase; Stator; Stator stalk; Peripheral stalk

1. Introduction

ATP synthase uses the energy contained in a transmembrane proton (or, in some bacteria, sodium ion) gradient to drive the synthesis of ATP from ADP and P_i. The enzyme is found in the inner membrane of mitochondria, the thylakoid membrane of chloroplasts, and the plasma membrane of bacteria, and is the central enzyme of energy metabolism in most organisms. In bacteria, under certain physiological conditions, ATP synthase runs in reverse, hydrolyzing ATP to generate a transmembrane proton gradient which is necessary for nutrient transport and locomotion. Proton translocation and ATP synthesis (or hydrolysis) are coupled by a unique mechanism, subunit rotation. Electrochemical energy contained in the proton gradient is converted into mechanical energy in form of subunit rotation, and back into chemical energy as ATP (for reviews, see Refs. [1–5]).

Traditionally, ATP synthase is divided into two subcomplexes, the membrane-embedded F_o subcomplex through which the protons flow, and the peripheral F_1 subcomplex that carries the nucleotide binding sites (Fig. 1). In the simplest form of the enzyme, in bacteria like *Escherichia coli*, F_1 consists of five different subunits, in a stoichiometry of $\alpha_3\beta_3\gamma\delta\varepsilon$; F_o consists of three different subunits, in a stoichiometry of ab_2c_{10-15} (for other organisms, see below). A newer, more mechanically-based division differentiates between the "rotor" (in *E. coli*, $\gamma\varepsilon c_n$) and the "stator" ($\alpha_3\beta_3\delta ab_2$). The $\alpha_3\beta_3$ ring of the stator contains the three catalytic nucleotide binding sites, on the β subunits at the interface to the adjacent α subunit. The *a* subunit contains the static portion of the proton-translocating machinery. $\alpha_3\beta_3$ and *a* are held together by the "stator stalk" (or "peripheral stalk"), consisting of $b_2\delta$. During rotation, the stator stalk experiences elastic strain, which has been estimated to be equivalent to about 50 kJ/mol [6,7]. The interaction between the individual components of the stator stalk have to be sufficiently strong to withstand the rotary strain. A high-resolution structure of the complete stator stalk is not available, although the structure of some fragments has been solved (see below).

Here, I will review the available information on the structure of the stator stalk, with specific emphasis on subunit arrangement and interactions with F_1. Many of the experimental results discussed in the following were obtained with bacterial ATP synthase. However, available information on differences and similarities of the mitochondrial or chloroplast enzymes will be included. (For earlier reviews on this topic, see Refs. [8–11]. I

* Tel.: +1 806 742 1297; fax: +1 806 742 1289.
E-mail address: joachim.weber@ttuhsc.edu.

0005-2728/$ - see front matter © 2006 Elsevier B.V. All rights reserved.
doi:10.1016/j.bbabio.2006.04.007

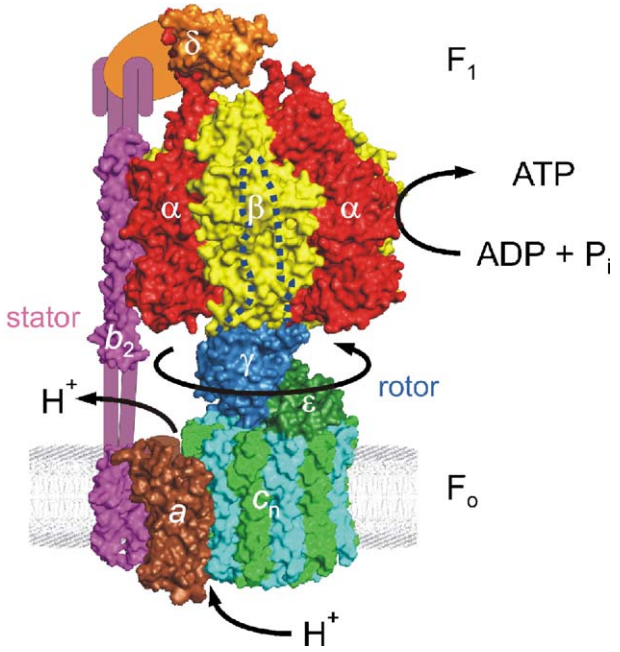

Fig. 1. Model of *Escherichia coli* ATP synthase. The model is a composite of structures obtained by X-ray crystallography [19,73], NMR [13,46,74], and modeling [74]. The rotor subunits ($\gamma\varepsilon c_n$) are in blue/green colors, the stator subunits ($\alpha_3\beta_3\delta a b_2$) in yellow and reddish hues. In comparison to earlier versions of the model (see e.g., [5]), the NMR structure of δ′ [23] was replaced by the structure of the δ′/αN1–22 complex [46]. Furthermore, the position of δ and structural aspects of the unresolved portions of the *b* dimer were changed to illustrate issues discussed in the text. All figures were generated using PyMOL [75].

would also like to point the reader's attention to another review in this issue that focuses on the stator stalk of the mitochondrial enzyme [12].)

2. Composition of the stator stalk and structure of its components

In *E. coli* (and other non-photosynthetic bacteria), the stator stalk consists of two copies of subunit *b* and one copy of subunit δ (Fig. 1). Subunit *b* has 156 residues. Its N-terminus is located on the periplasmic side of the membrane, immediately followed by a transmembrane helix. NMR studies of a peptide consisting of residues 1–34[1] show this helix, interrupted by a bend around residues 23–26, after which the helix resumes [13]. The cytoplasmic portion of the protein is actually predicted[2] to be a single helix, up to the C-terminus, with a potential short break (~4 residues) in the helix around residue 140. The elongated shape and largely α-helical character of the cytoplasmic domain of *b* ("b_{sol}"[3]), in dimeric form, were demonstrated experimentally by analytical ultracentrifugation and circular dichroism measurements, respectively [16]; in monomeric b_{sol}, the content of α-helix is reduced [17,18]. The crystal structure of a peptide corresponding to residues 62–122 showed a single, almost straight helix [19]. It is not precisely known how far up *b* has to reach at the side of F_1. If the cytoplasmic helix were fully extended, perpendicular to the plane of the membrane, it would reach far beyond the apex of F_1 (190 Å versus 135 Å from the surface of the membrane). In fact, there is evidence from analytical ultracentrifugation data on C-terminally truncated b_{sol} molecules that the extreme C-terminus is bent back in a hairpin-like fashion [20]; the turn could be located at the predicted break of the α-helix.

Despite its extended helical structure, the cytoplasmic portion of *b* (or of the *b* dimer) does not appear to be a stiff rod, but somewhat flexible, especially in the tether domain. Subunit *b* can tolerate deletions of up to 11 amino acids, corresponding to shortening the helix by 16 Å, or insertions of up to 14 amino acids, corresponding to lengthening the helix by 20 Å, under preservation of enzymatic function [21,22]. These findings suggest a certain flexibility in the cytoplasmic helix between its attachment points to F_o and F_1 [22]. An alternative, but by no means mutually exclusive, explanation would be to accommodate these length differences, at least partially, by reducing or increasing the angle of the bend between the transmembrane helix and the cytoplasmic helix.

Like the *b* subunits, δ is essential for a functional ATP synthase. The structure of the N-terminal domain (residues 2–106, out of a total of 177) has been solved by NMR [23], showing a six-helix bundle (Fig. 2). The C-terminal domain is less well ordered, at least in the isolated subunit [23]; however, it appears to be also largely helical [24]. The two natural Cys residues, δCys65 in the N-terminal domain and δCys141 in the C-terminal domain, have been proposed to be in rather close spatial proximity [25], which would give δ a rather compact overall structure. On the other hand, data from gel filtration experiments on isolated δ [26] and the proposed locations of its N- and C-termini relative to F_1 (see below) favor an elongated shape.

ATP synthases from cyanobacteria and other photosynthetic eubacteria as well as from chloroplasts contain two different types of *b* subunits, termed *b* and *b′* in cyanobacteria and subunits I and II in chloroplasts. Despite overall only weak homologies, these *b*-type subunits have a common predicted structure: an N-terminal transmembrane helix and an extended cytoplasmic (or, in the case of the chloroplast enzyme, stromal) helix. Like in *E. coli b*, in cyanobacterial (*Synechocystis*) *b* and in chloroplast (spinach) subunit I, this latter helix is about 130 residues long, with a predicted short interruption about 20 residues from the C-terminus. In Synechocystis *b′* and spinach subunit II, this helix is shorter (about 110 residues), with no

[1] Residue numbering refers to the E. coli enzyme. Residue numbers for subunit δ assume that the N-terminal Met is present. For *b*, the domain nomenclature suggested by Dunn et al. [8] will be used, which differentiates between the membrane domain (residues 1–23), the tether domain (24–53), the dimerization domain (54–122), and the C-terminal domain (123–156).

[2] Secondary structure predictions in the author's lab were made using the PredictProtein server (http://www.predictprotein.org/), programs PHD and PROF [14,15].

[3] Abbreviations: b_{sol} (=$b_{soluble}$), *b* constructs in which the transmembrane domain has been removed; it should be noted that there might be differences between b_{sol} constructs used in different studies. OSCP, oligomycin-sensitivity conferring protein; the mitochondrial equivalent of the bacterial (and chloroplast) δ subunit.

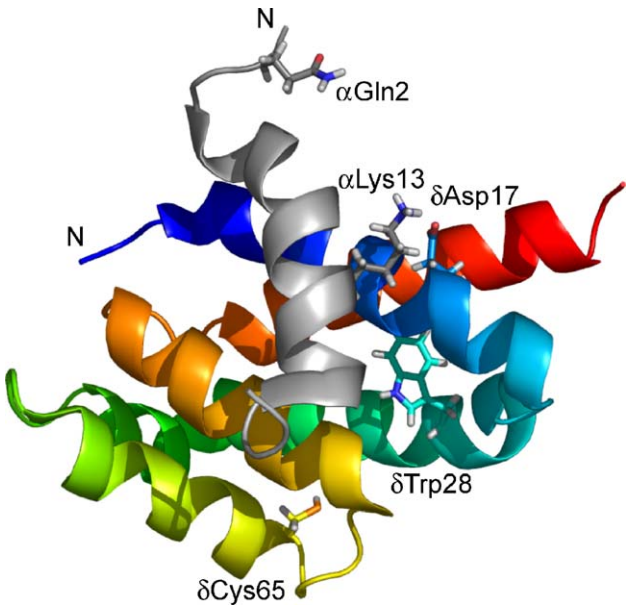

Fig. 2. Interaction of δ with the N-terminal helix of α. The NMR structure of a complex of δ′ with peptide αN1–22, mimicking residues 1–22 of α, is shown [46]. The N-terminal domain of δ is shown in rainbow colors, the peptide in gray. The N termini of both chains are marked. Highlighted residues are: δTrp28, which gives a fluorescence response to binding of the N-terminal helix of α; αGln2 and δCys65, indicating that the crosslink observed between δCys65 and a Cys residue introduced in position α2 [51] requires involvement of a second α subunit; αLys13 and δAsp17, which form the only obvious charged/polar interaction between both chains in the δ′/αN1–22 complex. For a depiction of the hydrophobic interactions, see Fig. 4B in [46].

predicted breaks. Thus, these subunits might be missing the proposed C-terminal hairpin-like structure of the longer *b*-type subunits (see above).

In mitochondrial ATP synthase, the stator stalk consists of at least 4 different subunits, each in a single copy: *b*, *d*, F_6, and OSCP [27,28]. Subunit *b* has only very weak, if any at all, homologies with the *b*-type subunits listed above; however, it appears to have a similar overall structure. The main difference is that mitochondrial *b* has two predicted transmembrane helices, suggesting a hairpin structure with the N-terminus in the mitochondrial matrix, on the side of F_1. The transmembrane segment is followed by an extended helical structure of about 140 residues, with a predicted short interruption in the helix about 30 residues from the C-terminus. Subunit *d* has no significant homologies with any *b*-type subunit. In bovine mitochondria, *d* has 161 residues. It has no predicted transmembrane helix, but is overall helical, although not in form of a single extended helix. Predictions propose 8 helices, the longest with about 31 residues. F_6 is a small protein (76 residues in bovine mitochondria), with no significant sequence similarities to any subunit of bacterial or chloroplast ATP synthases. The structure of F_6 has been solved by NMR. F_6 is highly flexible, consisting of two helixes, connected by an unstructured linker [29]. OSCP has significant homologies to bacterial and chloroplast δ subunits; in general, these δ-type subunits are more conserved than the b-type subunits. The structure of the N-terminal domain of OSCP has been solved by NMR [30], and it is very similar to the structure of the N-terminal domain of *E. coli* δ [23]. The main difference is in the surface charge, which is overall positive in OSCP and negative in *E. coli* δ [30].

3. Subunit–subunit interactions in the stator stalk: the *b* dimer

Most experimental data suggest that *E. coli b* dimerizes in a parallel, side-by-side arrangement, without significant offset. Crosslinks between (individually) introduced Cys residues were reported for the membrane portion as well as for the cytoplasmic portion, up to the C-terminus [13,17,31–33]. Many of these crosslinks could be formed in the holoenzyme [13,17,32]. Suspiciously absent are crosslinks in the stretch of *b* between the attachment points in F_0 and F_1, i.e., the tether domain and the N-terminus of the dimerization domain, up to residue 84. Crosslinks between residues 59, 60 and 62 were found with the isolated cytoplasmic portion of *b* [31,34]; however, those between residues 60 and 62 could not be detected in the F_1F_o holoenzyme [17,34]. Other arguments for a less close contact between both *b* subunits in this region are the findings (a) that the tether region (up to residue 53) does not contribute significantly to dimer formation in isolated b_{sol} [31], and (b) that it is possible to form a functional "asymmetric" dimer between a *b* subunit where residues 54 to 60 have been deleted and a *b* subunit where a repeat of these residues is inserted [35]. A recent attempt to measure the distance between both *b* monomers in this region came up with a somewhat surprising finding. Based on EPR measurements, Steigmiller et al. [34] determined that pairs of spin labels attached to Cys residues inserted in five different positions between 40 and 64 are in each case 29 Å apart from each other. Taking the crosslinking data obtained in the holoenzyme into account, the EPR data [34] would leave several possible scenarios for the structure of the *b* dimer in the tether region: (a) between the points of close contact in the transmembrane region and around residue 84, the two *b* subunits diverge to a distance of 19 Å around residue 40, run in parallel to (at least) residue 64, and then converge again; (b) the two *b* subunits have bulges where 15–20 residues are looped out, in one *b* subunit between the membrane domain and residue 40, in the other between residues 64 and 84, so that both helices can run side-by-side in the tether region, one shifted by 27 Å versus the other; (c) a combination of a smaller divergence with a smaller shift. None of these scenarios is easy to reconcile with existing models.

As far as the cytoplasmic portion of *b* is concerned, only the portion between residues 53 and 122 appears to contribute significant binding energy for dimer formation ("dimerization domain") [20,33]. It has been suggested that in this region, the two helices form a coiled coil with a right-handed superhelical twist [19]. Although crosslinking data suggest that also the C-termini of both *b* subunits come close to each other (see above), removing them did not change the affinity between two b_{sol} subunits [20]. The affinity is relatively weak; analytical ultracentrifugation gave K_d values of 1–2 μM [20,36]. However, it seems highly likely that the membrane domain contributes additional binding energy. At the very least, anchoring *b* in the membrane will increase the local concentration available for dimer formation.

As an example of organisms that have two different *b*-type subunits, the soluble portions of *b* and *b*′ of *Synechocystis* preferentially form a heterodimer, although a small amount of homodimer could be observed for each construct [18]. For the mitochondrial enzyme, the heterodimer consisting of b_{sol} and *d* as well as the heterotrimer consisting of b_{sol}, *d*, and F_6 were found stable enough to withstand gel filtration chromatography [24].

4. The interaction of *b* and δ

b binds to δ with its C-terminal domain. Removal of 4 residues from the C-terminus of *b* disrupted binding of δ, and Cys residues inserted at the C-terminus could be crosslinked to δ [37]. Likewise, the C-terminus of chloroplast subunit I could be crosslinked to δ [38]. In the case of δ, it is also the C-terminus that binds to *b*, as shown by crosslinking [37] and NMR studies [17]. In the case of the mitochondrial enzyme, deletion of the 10 C-terminal residues from OSCP prevented binding to F_o, probably by removing the C-terminal α-helix [39,40].

Analytical ultracentrifugation data showed that the complex formed between *E. coli* b_{sol} and δ has the stoichiometry $(b_{sol})_2\delta$. The *b* dimer and δ are probably arranged in an end-to-end, not in a side-by-side way [41]. Monomeric *b* appears to have a significantly lower affinity for δ than the dimeric form, as only the b_{sol} dimer, but not a monomer which included a mutation preventing dimerization was able to compete with intact F_o in reconstitution experiments [17]. Still, even the affinity of b_2 for δ is fairly weak. From NMR experiments, a K_d of >2 μM was estimated [17], analytical ultracentrifugation gave values of 5–10 μM [41]; it cannot be excluded, however, that after assembly into the holoenzyme these interactions are strengthened due to cooperative effects. In the mitochondrial enzyme the interactions seem to be somewhat tighter, as a complex between the monomeric mitochondrial b_{sol} and OSCP could be isolated by gel filtration chromatography; also a quaternary complex of b_{sol}, *d*, F_6, and OSCP could be obtained [27].

5. Binding of the stator stalk to F_1: interactions between δ and F_1

E. coli δ contains a single Trp residue, δTrp28, in the N-terminal domain at the beginning of helix 2. The fluorescence of this Trp increases by 50% upon binding of δ to δ-depleted F_1. Using this signal, a K_d of 1.4 nM was determined for the interaction between δ and δ-depleted F_1 [42]. Presence of b_{sol}, probably in the form of b_{sol} dimer, tightened binding between δ and F_1 further [43]. While technical limitations of the assay did not allow measurement of this effect with wild-type δ, it could be shown for several δ mutants with reduced affinity. In all cases investigated [43], in presence of b_{sol} binding of δ to δ-depleted F_1 was so tight that only an upper limit for the K_d could be estimated. From these data, we concluded that presence of b_{sol} increases the affinity between δ and F_1 by at least a factor of 500. For wild-type δ, this would result in a K_d of <3 pM.

Using fluorescence correlation spectroscopy and tetramethylrhodamine-labeled δ, also for the chloroplast enzyme a tight interaction between δ and F_1 was measured, with a K_d of ≤0.8 nM (in absence of *b*-type subunits) [44]. In contrast, the affinity of mitochondrial F_1 for OSCP appears to be somewhat lower ($K_d \approx 80$ nM [45]), which could explain that in the bacterial and chloroplast enzymes δ purifies as part of the F_1 subcomplex, while in the mitochondrial enzyme OSCP does not. The C-terminus of δ is not involved in binding to F_1, as a proteolytic fragment of *E. coli* δ, δ′, consisting of residues 1–134, bound with the same affinity as intact δ [42]. Mutagenesis results [43] and NMR data [30,46] demonstrated that the major interaction surface with F_1 consists of helices 1 and 5 in the N-terminal domain of δ (Fig. 2) or, in the case of the mitochondrial enzyme, of OSCP.

For a long time, it had been suggested that the extreme N-terminus of α is the site where F_1 interacts with δ. Proteolytic removal of the first 19 residues from α greatly reduced binding of δ [47]. In the available crystal structures of F_1, the extreme N-terminus of α, i.e., the portion that extends beyond the "crown" region of the $\alpha_3\beta_3$ ring, is not completely resolved; in one case [48], a helix-like structure can be seen between residues 13, the first resolved residue, and the crown region at around residue 24. Secondary structure predictions suggested that the N-terminus of α forms a helix between residues 6 and 18 [49]. NMR analysis of a complex between δ′ and a peptide corresponding to residues 1–22 of α (termed "αN1–22") demonstrated the helical structure of α between residues 4 and 19 [46], at least in the δ-bound state. Circular dichroism measurements of the free (unbound) peptide gave a helix content of about 25% [49], indicating that binding to δ leads to an increase in ordered, helical structure. As a modification of earlier models for α/δ interaction, which had the N-terminal helix of α run in a groove between helices 1 and 5 of δ and parallel (or antiparallel) to them [30,50], the NMR data showed an angle of ~ 45 ° between the N-terminal helix of α and the two helices in δ (Fig. 2). Interaction forces are largely hydrophobic, the exception being a salt bridge/hydrogen bond between the side chains of residues αLys13 and δAsp17. The structure of the N-terminal domain of δ does not show significant changes upon binding to the α peptide [46]. As the attachment of the N-terminal helix of α to the crown domain is probably rather flexible, details of the conformational arrangement of the N-terminal domain of δ with regard to the bulk of F_1 are still open.

In fluorescence titrations with δ, the αN1–22 peptide mimicked F_1 very well [49]. Upon saturation with peptide, the fluorescence response of δTrp28 was the same as observed upon saturation with δ-depleted F_1. The NMR structure of the δ′/αN1–22 complex indicated no direct interaction between the peptide and δTrp28 (Fig. 2); however, there are subtle changes in the environment of the indole ring of the Trp, which might account for the increased quantum yield. The affinity of δ for the αN1–22 peptide was somewhat reduced, with a K_d of 130 nM, as compared to 1.4 nM for δ-depleted F_1. Still, this means that the major portion of the binding energy (>75%) between F_1 and δ is supplied by the N-terminal helix of one of the three α subunits. The interactions that contribute the additional binding energy have not yet been identified. An interesting speculation is based on comparison of the NMR structure of the δ′/αN1–22 complex with crosslinking data [51] that

describe disulfide bonds between a Cys introduced in position 2 of α and both natural Cys residues in δ. As can be seen from Fig. 2, disulfide bond formation between residue 2 of the αN1–22 helix and residue δCys65 is virtually impossible. Thus, it could be the N-terminal helix of one of the other two α subunits that comes in close contact with δCys65 and contributes some small amount of binding energy. This would position the N-terminal domain of δ on "top" of F_1. Steric hindrances would explain why, despite the presence of 3 potential binding sites (one per α N-terminus) of rather high individual mobility, only one δ binds per F_1 [42] (although for OSCP the existence of additional, lower-affinity binding sites was suggested [30,45]). A location of δ on top of F_1 had been proposed on the basis of immuno electron microscopy [52], although in that case the antibody used for immunodecoration supposedly recognized the C-terminal domain of δ [53]. This brings the results of [52] in contrast to those obtained in a electron microscopy study on OSCP [54], which placed the C-terminus of OSCP on the "side" of F_1, approximately at the transition region between the N-terminal crown domain and the central nucleotide binding domain.

Another observation that favors a restriction of the δ/F_1 contact sites largely to the interaction sites between the N-terminal domain of δ and the extreme N-terminus of one or more α subunits is described in [42]. In these experiments, Trp residues had been inserted into the N-terminal crown domain of F_1, in positions α55, β17, and β26 (see Fig. 3). None of these Trp residues showed a fluorescence response upon binding of δ; neither did the "natural" βTrp107, which is located at the top of the central nucleotide binding domain. Originally, this finding was ascribed to the rigidity of F_1 in this region, which would leave the environment of each of these residues unchanged if δ was present or not. However, subsequently [55] we noticed that three of the four residues (αTrp55, βTrp26, βTrp107) respond to the binding of b_{sol} (see below and Fig. 3), showing that it was not rigidity, but in all likelihood absence of significant contact between δ and these regions of F_1 that prevented changes of the fluorescence signals in presence of δ.

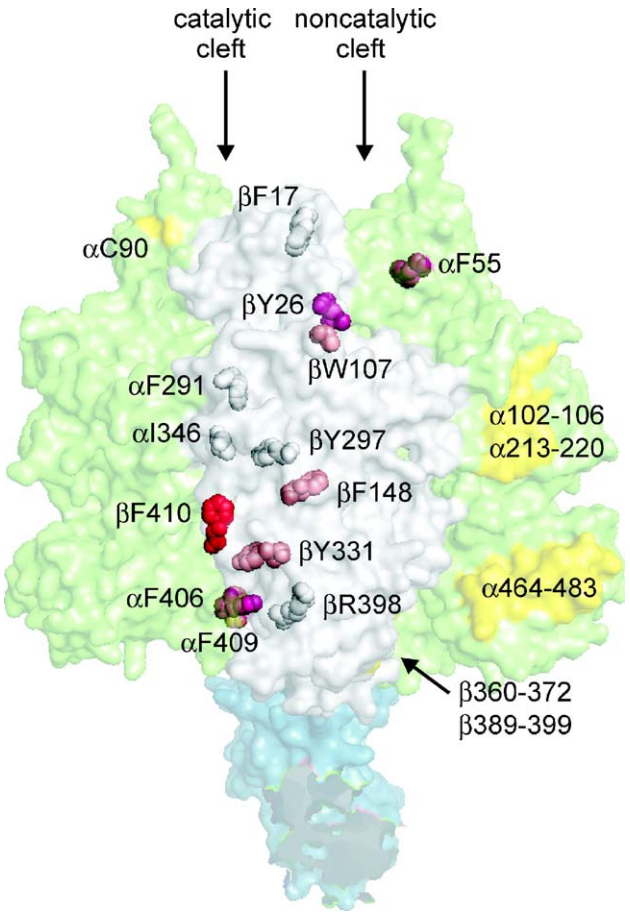

Fig. 3. Localization of the stator stalk. F_1 (minus δ and ε) is shown in a side view as a transparent surface, with α in green, β in grey, and γ in blue. Highlighted in "spacefill" representation are residues in positions where an inserted Trp was analyzed with regard to its fluorescence response upon binding of *b* [55]. The strength of the response is indicated by the color of the residue, ranging from white (no response) via different shades of pink to red (>20% signal increase). Areas that can be reached by crosslinking from *b* [32,56] are indicated as yellow surfaces. The location of an additional area [56] that is hidden from view is indicated by the arrow. Suggested positions for the stator stalk based on electron microscopy are discussed in the text.

6. Binding of the stator stalk to F_1: interactions between *b* and F_1

Crosslinking experiments [32,56] and spin-labeling data [57,58] had indicated that *b* binds to F_1 not only via δ, but also directly to α and/or β. Recently, two studies attempted to quantify the interactions between *b* and F_1 [36,55]. In one of those [55], we investigated the fluorescence signal of more than 10 Trp residues in different regions of α and β upon addition of b_{sol}. More than 60% responded with a fluorescence increase (Fig. 3). On average, the response of Trp residues closer to the outer surface of F_1 was larger than that of residues in the interior. Somewhat unexpected was the response of residues αTrp406 and αTrp409 which are relatively near to the protein surface, but "under" the $\alpha_3\beta_3$ ring, closer to the central stalk and the rotation axis. The largest fluorescence increase, 24%, was observed for βTrp410; assuming that only one of the three Trp residues in this position reacts to binding of b_{sol}, this would mean a signal increase by 72% for this residue. Except for differences in amplitude, all titration curves had a similar shape. Assuming that all b_{sol} was present in dimer form, in presence of Mg^{2+} an apparent K_d for binding of $(b_{sol})_2$ to F_1 of around 100 nM was obtained [55]. In absence of Mg^{2+} and presence of EDTA, the affinity was weaker, by a factor of 10, which could explain why F_1 is released from *E. coli* membranes in absence of divalent cations.

Diez et al. [36] measured the affinity between fluorescence-labeled F_1 and b_{sol} by fluorescence correlation spectroscopy and by steady-state fluorescence resonance energy transfer. Taking into account the differences in experimental set-up, the titration curves based on the energy transfer data were comparable to those in [55]. However, the evaluation in [36] took the rather weak affinity for *b* dimer formation (K_d = 1.8 μM) into account, and obtained for binding of $(b_{sol})_2$ to F_1 a K_d of between 0.6 and 14 nM, depending on the binding model. The former value

roughly agreed with the K_d of 0.2 nM determined by fluorescence correlation spectroscopy [36]. In a subsequent study, using full-length *b* incorporated into proteoliposomes and single molecule resonance energy transfer, a K_d of about 10 nM was found for binding of *b* dimer to F_1 [59].

It should be emphasized that all these values were obtained in binding experiments with intact, five-subunit F_1. This means, F_1 still contained the δ subunit, and the measured affinities are based on interactions between *b* and δ as well as between *b* and $\alpha_3\beta_3$. When we studied binding of b_{sol} to δ-depleted F_1, we saw no effect of δ-depletion on the binding affinity [55]. This was unexpected, as interaction between *b* and δ is essential for enzymatic function (ATP synthesis, ATP-driven proton pumping, ATP-P_i exchange) [8,37,39,42], and created a thermodynamic dilemma in consideration of the strong effect of b_{sol} on the affinity between δ and F_1 (see above). However, recent simulations (not shown) indicated that, under the given conditions and taking the *b* monomer–dimer equilibrium into account, the assay system may have been at its limits; decreasing the K_d for the interaction between $(b_{sol})_2$ and F_1 beyond 1 nM had little effect on the overall binding curves. Thus, the question of the influence of δ on the binding affinity between *b* and F_1 remains open.

Data on binding of individual, monomeric *b* subunits to F_1 are scarce. Reconstitution competition experiments, using a dimerization-impaired *b* mutant, indicated that the monomer has no significant affinity [60]. For the mitochondrial enzyme, in absence of OSCP, the single *b* subunit did not form a complex with F_1 that was stable enough to withstand gel filtration chromatography; in presence of OSCP, a complex was observed, but *b* appeared to be present in substoichiometric amounts [27]. On the other hand, thermodynamic considerations dictate that, if K_1 is the dissociation constant for binding of the first *b* monomer to F_1, K_2 is that for binding of the second *b* to the F_1b_1 complex, K_3 is the K_d for dimerization of *b*, and K_4 is the K_d for binding of b_2 to F_1, then

$$K_1K_2 = K_3K_4 \quad (1)$$

Using this dependency in the evaluation of their energy transfer data, Diez et al. [36] found the best fits for K_1 values of 30–50 nM and K_2 values of 30–500 nM, depending on the binding model. Thus, especially for the first step, binding of a b_{sol} monomer to F_1, the affinity is fairly high. It should be noted that this evaluation still contains an oversimplification, and that is the assumption that K_1 for binding of *b* in one of the possible positions on F_1 is the same as K_1 for binding of *b* in the other possible position. Symmetry considerations impose that both monomers in a *b* dimer have different interactions with F_1.[4]

The position of the stator stalk, particularly the *b* dimer, with regard to the $\alpha_3\beta_3$ ring is controversial. An early cryoelectron microscopy study [62], using immunodecorated α subunits as reference points, positioned the stator stalk of the *E. coli* enzyme on the outer surface of one of the β subunits. Subsequent cryoelectron microscopy studies modeled F_1 crystal structures into the electron microscopy map and used those as reference. They found the stator stalk of the chloroplast enzyme outside of an α subunit [63], and that of the mitochondrial enzyme in a noncatalytic cleft [64]. It seems highly unlikely that the position of the stator stalk should be species-dependent. Crosslinking, using the *E. coli* enzyme, located the central region of *b* (around residue 100) in the lower half of the $\alpha_3\beta_3$ ring in a noncatalytic cleft [56] and the C-terminus near to residue αCys90, close to the top of the N-terminal crown domain at a catalytic cleft [32]. We had hoped that the location of the Trp residues that gave a response to binding of b_{sol} ([55] and Fig. 3) might give additional information about the location of the stator stalk; however, the results were inconclusive. In the C-terminal and central domains, βTrp 410 and αTrp406, both of which are located close to the catalytic cleft, gave the strongest response. On the other hand, in the N-terminal domain two residues close to the noncatalytic cleft, βTrp26 and αTrp55 showed a pronounced increase in their fluorescence signals (Fig. 3). In retrospect, these results are certainly biased by the distribution of the Trp residues included in this study. Overall, the data seem to indicate long-range conformational changes in F_1, which might be rather subtle, due to binding of *b* (see also Ref. [57]). This makes the absence of responses by the Trp residues in the N-terminal domain to binding of δ, which was discussed above, even more remarkable.

7. Binding of the stator stalk to F_o: interactions between *b* and *a*

The interaction between subunits *a* and *b* is less well defined, from an energetic as well as from a structural point of view. In absence of affinities measurements, the strongest argument for a tight interaction between *a* and *b* is the demonstration that it is possible to purify an ab_2 complex that, using a His-tagged *a* subunit, was stable enough to withstand affinity chromatography in different detergents and detergent mixtures [65]. It is not known if just one or both of the *b* subunits contact(s) *a*. Second site revertants for the mutation *b*G9D were found in position *a*240 [66], which is located in the C-terminal of the five putative transmembrane helices of *a* [67,68]. However, according to a recent model of the transmembrane helix arrangement of the ab_2 complex [69], the suppressor effect is indirect and transmitted via helix 2 of *a*. The model [69] places one of the transmembrane helices of the *b* dimer adjacent to helices 1 and 2 of *a*, the other just close to helix 2. This model is supported by the finding that a Cys residue inserted in the rather long cytoplasmic loop between transmembrane helices 1 and 2 of *a* could be crosslinked to subunit *b* [70]. Together with the demonstration that a Cys introduced in position *b*36, i.e., a few turns into the predicted cytoplasmic helix of *b*, could be crosslinked to *a* [56], these data show that the contact between *a* and *b* is not restricted to the immediate membrane region.

8. Conclusions: subunit interactions and function of the stator stalk

Certainly, it would be very desirable to have a high resolution structure of the stator stalk or, even better, of the ATP

[4] The functional non-equivalence of the two *b* subunits in the *E. coli* enzyme has recently been shown experimentally [61].

synthase holoenzyme. Despite the absence of a breakthrough of this dimension, steady progress has been made in recent years towards a coherent picture of the structure of the stator stalk, especially with regard to the attachment of the stator stalk to F_1 and to quantitative analysis of subunit–subunit interactions.

The current knowledge about the structure of the stator stalk can be summarized as follows: A model of the major attachment point between *E. coli* subunits δ and α has been derived [46], and the structure of the interaction site between OSCP and α in the mitochondrial enzyme appears to be similar [30]. One or more additional minor interaction sites between these subunits seem to exist whose location is unknown, except for the finding that the C-terminal portion of δ is not involved [42]. δ and *b* interact with their C-terminal domains [37–40], but molecular details of the contact site are not yet known. The structure of the dimerization domain of *b* has been resolved [19], although it has been questioned if the N-terminal portion of this domain has the same structure after assembly of the *b* dimer into the holoenzyme [34]. The location of the interaction site of the *b* dimer with the $\alpha_3\beta_3$ ring is uncertain; however, the noncatalytic interface seems to be favored [56,64]. The conformation of the *b* dimer in the tether domain is unresolved, but it is possibly rather flexible [21,22,35]. The structure of the transmembrane domain of a *b* monomer has been resolved, and a model for the dimer was presented [13]. The interaction sites between the *b* dimer and *a* are not well defined.

The function of the peripheral stalk is to hold the stator portions of the machineries for ATP synthesis/hydrolysis and proton translocation together during subunit rotation. The stator stalk has to withstand elastic strain because the stepping angles of the F_1 motor and the F_o motor are different, 120 ° per ATP in F_1 and (360/n) ° per proton in F_o, with n being the number of *c* subunits (n = 10–15, depending on organism). Based on mechanical considerations (torque × angular displacement) [44] or on the free energy necessary for ATP synthesis [36], the elastic strain has been estimated as equivalent to 50–55 kJ/mol. As pointed out in [36], the elastic strain can become smaller if the energy transduction between both motors occurs in substeps, as long as strain is released after each substep. And indeed, it has been shown that rotation occurs in two substeps of 80 ° and 40 ° [71,72], each one associated with partial reactions of the catalytic cycle [4,71,72]. It is, however, not known to what extent the elastic strain is released after each substep.

A K_d of 1 nM corresponds to a free energy of binding of about 50 kJ/mol. Thus, in presence of *b*, with an estimated K_d in the pM range [43], δ binds clearly tightly enough to F_1 to withstand the elastic strain even if the energy transmission occurred in a single step. It is, however, the interaction between the *b* dimer and F_1 that is critical to hold the stator parts together, consisting of the contacts with δ as well as those directly with the $\alpha_3\beta_3$ ring. In this case, with affinities in the nM range, only an energy transduction in substeps appears to provide a sufficiently large safety margin [36]. A reason for concern could be the low concentration of available *b* dimer, in case of an unfavorable monomer–dimer equilibrium. However, as discussed above, the measured (relatively high) K_d values [20,36] were obtained using b_{sol}. For full-length *b*, in a membrane environment, it is highly likely that the equilibrium is more on the side of the dimer. For the interaction between the stator stalk with F_o, i.e., between *b* dimer and *a*, no affinity data are available; nevertheless, it seems reasonably stable [65].

Acknowledgements

Work in the author's lab is supported by NIH grant GM071462.

References

[1] D. Stock, C. Gibbons, I. Arechaga, A.G.W. Leslie, J.E. Walker, The rotary mechanism of ATP synthase, Curr. Opin. Struct. Biol. 10 (2000) 672–679.
[2] H. Noji, M. Yoshida, The rotary machine in the cell, ATP synthase, J. Biol. Chem. 276 (2001) 1665–1668.
[3] R.A. Capaldi, R. Aggeler, Mechanism of the F_1F_0-type ATP synthase, a biological rotary motor, Trends Biochem. Sci. 27 (2002) 154–160.
[4] A.E. Senior, S. Nadanaciva, J. Weber, The molecular mechanism of ATP synthesis by F_1F_0-ATP synthase, Biochim. Biophys. Acta 1553 (2002) 188–211.
[5] J. Weber, A.E. Senior, ATP synthesis driven by proton transport in F_1F_0-ATP synthase, FEBS Lett. 545 (2003) 61–70.
[6] R. Yasuda, H. Noji, K. Kinosita Jr., M. Yoshida, F_1-ATPase is a highly efficient molecular motor that rotates with discrete 120 degree steps, Cell 93 (1998) 1117–1124.
[7] O. Pänke, D.A. Cherepanov, K. Gumbiowski, S. Engelbrecht, W. Junge, Viscoelastic dynamics of actin filaments coupled to rotary F-ATPase: angular torque profile of the enzyme, Biophys. J. 81 (2001) 1220–1233.
[8] S.D. Dunn, D.T. McLachlin, M. Revington, The second stalk of *Escherichia coli* ATP synthase, Biochim. Biophys. Acta 1458 (2000) 356–363.
[9] S.D. Dunn, M. Revington, D.J. Cipriano, B.H. Shilton, The *b* subunit of *Escherichia coli* ATP synthase, J. Bioenerg. Biomembr. 32 (2000) 347–355.
[10] J.C. Greie, G. Deckers-Hebestreit, K. Altendorf, Subunit organization of the stator part of the F_0 complex from *Escherichia coli* ATP synthase, J. Bioenerg. Biomembr. 32 (2000) 357–364.
[11] B.D. Cain, Mutagenic analysis of the F_0 stator subunits, J. Bioenerg. Biomembr. 32 (2000) 365–371.
[12] J.E. Walker, V.K. Dickson, The peripheral stalk of the mitochondrial ATP synthase, Biochim. Biophys. Acta (2006), doi:10.1016/j.bbabio.2006.01.001 (this issue).
[13] O. Dmitriev, P.C. Jones, W. Jiang, R.H. Fillingame, Structure of the membrane domain of subunit *b* of the *Escherichia coli* F_0F_1 ATP synthase, J. Biol. Chem. 274 (1999) 15598–15604.
[14] B. Rost, PHD: predicting one-dimensional protein structure by profile-based neural networks, Methods Enzymol. 266 (1996) 525–539.
[15] B. Rost, R. Casadio, P. Fariselli, C. Sander, Transmembrane helices predicted at 95% accuracy, Protein Sci. 4 (1995) 521–533.
[16] S.D. Dunn, The polar domain of the *b* subunit of *Escherichia coli* F_1F_0-ATPase forms an elongated dimer that interacts with the F_1 sector, J. Biol. Chem. 267 (1992) 7630–7636.
[17] A.J.W. Rodgers, S. Wilkens, R. Aggeler, M.B. Morris, S.M. Howitt, R.A. Capaldi, The subunit δ-subunit *b* domain of the *Escherichia coli* F_1F_0 ATPase. The *b* subunits interact with F_1 as a dimer and through the δ subunit, J. Biol. Chem. 272 (1997) 31058–31064.
[18] S.D. Dunn, E. Kellner, H. Lill, Specific heterodimer formation by the cytoplasmic domains of the *b* and *b′* subunits of cyanobacterial ATP synthase, Biochemistry 40 (2001) 187–192.
[19] P.A. Del Rizzo, Y. Bi, S.D. Dunn, B.H. Shilton, The "second stalk" of *Escherichia coli* ATP synthase: structure of the isolated dimerization domain, Biochemistry 42 (2002) 6875–6884.
[20] M. Revington, S.D. Dunn, G.S. Shaw, Folding and stability of the *b* subunit of the F_1F_0 ATP synthase, Protein Sci. 11 (2002) 1227–1238.
[21] P.L. Sorgen, T.L. Caviston, R.C. Perry, B.D. Cain, Deletions in the second stalk of F_1F_0-ATP synthase in *Escherichia coli*, J. Biol. Chem. 273 (1998) 27873–27878.

[22] P.L. Sorgen, M.R. Bubb, B.D. Cain, Lengthening the second stalk of F_1F_0 ATP synthase in *Escherichia coli*, J. Biol. Chem. 274 (1999) 36261–36266.
[23] S. Wilkens, S.D. Dunn, J. Chandler, F.W. Dahlquist, R.A. Capaldi, Solution structure of the N-terminal domain of the δ subunit of the *E. coli* ATP synthase, Nat. Struct. Biol. 4 (1997) 198–201.
[24] S. Engelbrecht, J. Reed, F. Penin, D.C. Gautheron, W. Junge, Subunit δ of chloroplast F_0F_1-ATPase and OSCP of mitochondrial F_0F_1-ATPase: a comparison by CD-spectroscopy, Z. Naturforsch. [C] 46 (1991) 759–764.
[25] M. Ziegler, R. Xiao, H.S. Penefsky, Close proximity of Cys64 and Cys140 in the δ subunit of *Escherichia coli* F_1-ATPase, J. Biol. Chem. 269 (1994) 4233–4239.
[26] P.C. Sternweis, J.B. Smith, Characterization of the purified membrane attachment (δ) subunit of the proton translocating adenosine triphosphatase from *Escherichia coli*, Biochemistry 16 (1977) 4020–4025.
[27] I.R. Collinson, M.J. van Raaij, M.J. Runswick, I.M. Fearnley, J.M. Skehel, G.L. Orriss, B. Miroux, J.E. Walker, ATP synthase from bovine heart mitochondria. In vitro assembly of a stalk complex in the presence of F_1-ATPase and in its absence, J. Mol. Biol. 242 (1994) 408–421.
[28] I.R. Collinson, J.M. Skehel, I.M. Fearnley, M.J. Runswick, J.E. Walker, The F_1F_0-ATPase complex from bovine heart mitochondria: the molar ratio of the subunits in the stalk region linking the F_1 and F_0 domains, Biochemistry 35 (1996) 12640–12646.
[29] R.J. Carbajo, J.A. Silvester, M.J. Runswick, J.E. Walker, D. Neuhaus, Solution structure of subunit F_6 from the peripheral stalk region of ATP synthase from bovine heart mitochondria, J. Mol. Biol. 342 (2004) 593–603.
[30] R.J. Carbajo, F.A. Kellas, M.J. Runswick, M.G. Montgomery, J.E. Walker, D. Neuhaus, Structure of the F_1-binding domain of the stator of bovine F_1F_o-ATPase and how it binds an α subunit, J. Mol. Biol. 351 (2005) 824–838.
[31] D.T. McLachlin, S.D. Dunn, Dimerization interactions of the *b* subunit of the *Escherichia coli* F_1F_0-ATPase, J. Biol. Chem. 272 (1997) 21233–21239.
[32] A.J.W. Rodgers, R.A. Capaldi, The second stalk composed of the *b*- and δ-subunits connects F_0 to F_1 via an α-subunit in the *Escherichia coli* ATP synthase, J. Biol. Chem. 273 (1998) 29406–29410.
[33] M. Revington, D.T. McLachlin, G.S. Shaw, S.D. Dunn, The dimerization domain of the *b* subunit of the *Escherichia coli* F_1F_0-ATPase, J. Biol. Chem. 274 (1999) 31094–31101.
[34] S. Steigmiller, M. Börsch, P. Gräber, M. Huber, Distances between the *b*-subunits in the tether domain of F_0F_1-ATP synthase from *E. coli*, Biochim. Biophys. Acta 1708 (2005) 143–153.
[35] T.B. Grabar, B.D. Cain, Integration of *b* subunits of unequal lengths into F_1F_0-ATP synthase, J. Biol. Chem. 278 (2003) 34751–34756.
[36] M. Diez, M. Börsch, B. Zimmermann, P. Turina, S.D. Dunn, P. Gräber, Binding of the *b*-subunit in the ATP synthase from *Escherichia coli*, Biochemistry 43 (2004) 1054–1064.
[37] D.T. McLachlin, J.A. Bestard, S.D. Dunn, The *b* and δ subunits of the *Escherichia coli* ATP synthase interact via residues in their C-terminal regions, J. Biol. Chem. 273 (1998) 15162–15168.
[38] G. Beckers, R.J. Berzborn, H. Strotmann, Zero-length crosslinking between subunits δ and I of the H^+-translocating ATPase of chloroplasts, Biochim. Biophys. Acta. 1101 (1992) 97–104.
[39] S. Joshi, G.J. Cao, C. Nath, J. Shah, Oligomycin sensitivity conferring protein of mitochondrial ATP synthase: deletions in the N-terminal end cause defects in interactions with F_1, while deletions in the C-terminal end cause defects in interactions with F_0, Biochemistry 35 (1996) 12094–12103.
[40] S. Joshi, G.J. Cao, C. Nath, J. Shah, Oligomycin sensitivity conferring protein (OSCP) of bovine heart mitochondrial ATP synthase: high-affinity OSCP-F_o interactions require a local α-helix at the C-terminal end of the subunit, Biochemistry 36 (1997) 10936–10943.
[41] S.D. Dunn, J. Chandler, Characterization of a $b_2\delta$ complex from *Escherichia coli* ATP synthase, J. Biol. Chem. 273 (1998) 8646–8651.
[42] J. Weber, S. Wilke-Mounts, A.E. Senior, Quantitative determination of binding affinity of δ subunit in *Escherichia coli* F_1-ATPase: effects of mutation, Mg^{2+}, and pH on K_d, J. Biol. Chem. 277 (2002) 18390–18396.
[43] J. Weber, S. Wilke-Mounts, A.E. Senior, Identification of the F_1-binding surface on the δ subunit of ATP synthase, J. Biol. Chem. 278 (2003) 13409–13416.
[44] K. Häsler, O. Pänke, W. Junge, On the stator of rotary ATP synthase: the binding strength of subunit δ to $(\alpha\beta)_3$ as determined by fluorescence correlation spectroscopy, Biochemistry 38 (1999) 13759–13765.
[45] A. Dupuis, J.P. Issartel, J. Lunardi, M. Satre, P.V. Vignais, Interactions between the oligomycin sensitivity conferring protein (OSCP) and beef heart mitochondrial F_1-ATPase. 1. Study of the binding parameters with a chemically radiolabeled OSCP, Biochemistry 24 (1985) 728–733.
[46] S. Wilkens, D. Borchardt, J. Weber, A.E. Senior, Structural characterization of the interaction of the δ and α subunits of the *Escherichia coli* F_1F_0-ATP synthase by NMR spectroscopy, Biochemistry 44 (2005) 11786–11794.
[47] S.D. Dunn, L.A. Heppel, C.S. Fullmer, The NH_2-terminal portion of the α subunit of *Escherichia coli* F_1 ATPase is required for binding the δ subunit, J. Biol. Chem. 255 (1980) 6891–6896.
[48] R. Kagawa, M.G. Montgomery, K. Braig, A.G.W. Leslie, J.E. Walker, The structure of bovine F_1-ATPase inhibited by ADP and beryllium fluoride, EMBO J. 23 (2004) 2734–2744.
[49] J. Weber, A. Muharemagic, S. Wilke-Mounts, A.E. Senior, F_1F_0-ATP synthase. Binding of δ subunit to a 22-residue peptide mimicking the N-terminal region of α subunit, J. Biol. Chem. 278 (2003) 13623–13626.
[50] J. Weber, A. Muharemagic, S. Wilke-Mounts, A.E. Senior, Analysis of sequence determinants of F_1F_o-ATP synthase in the N-terminal region of α subunit for binding of δ subunit, J. Biol. Chem. 279 (2004) 25673–25679.
[51] I. Ogilvie, R. Aggeler, R.A. Capaldi, Cross-linking of the δ subunit to one of the three α subunits has no effect on functioning, as expected if δ is a part of the stator that links the F_1 and F_0 parts of the *Escherichia coli* ATP synthase, J. Biol. Chem. 272 (1997) 16652–16656.
[52] S. Wilkens, J. Zhou, R. Nakayama, S.D. Dunn, R.A. Capaldi, Localization of the δ subunit in the *Escherichia coli* F_1F_0-ATPsynthase by immuno electron microscopy: the δ subunit binds on top of the F_1, J. Mol. Biol. 295 (2000) 387–391.
[53] S.D. Dunn, R.G. Tozer, Activation and inhibition of the *Escherichia coli* F_1-ATPase by monoclonal antibodies which recognize the ε subunit, Arch. Biochem. Biophys. 253 (1987) 73–80.
[54] J.L. Rubinstein, J.E. Walker, ATP synthase from *Saccharomyces cerevisiae*: location of the OSCP subunit in the peripheral stalk region, J. Mol. Biol. 321 (2002) 613–619.
[55] J. Weber, S. Wilke-Mounts, S. Nadanaciva, A.E. Senior, Quantitative determination of direct binding of *b* subunit to F_1 in *Escherichia coli* F_1F_0-ATP synthase, J. Biol. Chem. 279 (2004) 11253–11258.
[56] D.T. McLachlin, A.M. Coveny, S.M. Clark, S.D. Dunn, Site-directed cross-linking of *b* to the α, β, and *a* subunits of the *Escherichia coli* ATP synthase, J. Biol. Chem. 275 (2000) 17571–17577.
[57] M.V. Kersten, S.D. Dunn, J.G. Wise, P.D. Vogel, Site-directed spin-labeling of the catalytic sites yields insight into structural changes within the F_0F_1-ATP synthase of *Escherichia coli*, Biochemistry 39 (2000) 3856–3860.
[58] C. Motz, T. Hornung, M. Kersten, D.T. McLachlin, S.D. Dunn, J.G. Wise, P.D. Vogel, The subunit *b* dimer of the F_OF_1-ATP synthase: interaction with F_1-ATPase as deduced by site-specific spin-labeling, J. Biol. Chem. 279 (2004) 49074–49081.
[59] T. Krebstakies, B. Zimmermann, P. Gräber, K. Altendorf, M. Börsch, J.C. Greie, Both rotor and stator subunits are necessary for efficient binding of F_1 to F_0 in functionally assembled *Escherichia coli* ATP synthase, J. Biol. Chem. 280 (2005) 33338–33345.
[60] P.L. Sorgen, M.R. Bubb, K.A. McCormick, A.S. Edison, B.D. Cain, Formation of the *b* subunit dimer is necessary for interaction with F_1-ATPase, Biochemistry 37 (1998) 923–932.
[61] T.B. Grabar, B.D. Cain, Genetic complementation between mutant *b* subunits in F_1F_0 ATP synthase, J. Biol. Chem. 279 (2004) 31205–31211.
[62] S. Wilkens, S.D. Dunn, R.A. Capaldi, A cryoelectron microscopy study of the interaction of the *Escherichia coli* F_1-ATPase with subunit *b* dimer, FEBS Lett. 354 (1994) 37–40.
[63] C. Mellwig, B. Böttcher, A unique resting position of the ATP-synthase from chloroplasts, J. Biol. Chem. 278 (2003) 18544–18549.

[64] J.L. Rubinstein, J.E. Walker, R. Henderson, Structure of the mitochondrial ATP synthase by electron cryomicroscopy, EMBO J. 22 (2003) 6182–6192.
[65] W.D. Stalz, J.C. Greie, G. Deckers-Hebestreit, K. Altendorf, Direct interaction of subunits *a* and *b* of the F_0 complex of *Escherichia coli* ATP synthase by forming an ab_2 subcomplex, J. Biol. Chem. 278 (2003) 27068–27071.
[66] C.A. Kumamoto, R.D. Simoni, Genetic evidence for interaction between the *a* and *b* subunits of the F_0 portion of the *Escherichia coli* proton translocating ATPase, J. Biol. Chem. 261 (1986) 10037–10042.
[67] J.C. Long, S. Wang, S.B. Vik, Membrane topology of subunit *a* of the F_1F_0 ATP synthase as determined by labeling of unique cysteine residues, J. Biol. Chem. 273 (1998) 16235–16240.
[68] F.I. Valiyaveetil, R.H. Fillingame, Transmembrane topography of subunit *a* in the *Escherichia coli* F_1F_0 ATP synthase, J. Biol. Chem. 273 (1998) 16241–16247.
[69] J. DeLeon-Rangel, D. Zhang, S.B. Vik, The role of transmembrane span 2 in the structure and function of subunit *a* of the ATP synthase from *Escherichia coli*, Arch. Biochem. Biophys. 418 (2003) 55–62.
[70] J.C. Long, J. DeLeon-Rangel, S.B. Vik, Characterization of the first cytoplasmic loop of subunit *a* of the *Escherichia coli* ATP synthase by surface labeling, cross-linking, and mutagenesis, J. Biol. Chem. 277 (2002) 27288–27293.
[71] R. Yasuda, H. Noji, M. Yoshida, K. Kinosita Jr., H. Itoh, Resolution of distinct rotational substeps by submillisecond kinetic analysis of F_1-ATPase, Nature 410 (2001) 898–904.
[72] K. Shimabukuro, R. Yasuda, E. Muneyuki, K.Y. Hara, K. Kinosita Jr., M. Yoshida, Catalysis and rotation of F_1 motor: cleavage of ATP at the catalytic site occurs in 1 ms before 40 degree substep rotation, Proc. Natl. Acad. Sci. U. S. A. 100 (2003) 14731–14736.
[73] C. Gibbons, M.G. Montgomery, A.G.W. Leslie, J.E. Walker, The structure of the central stalk in bovine F_1-ATPase at 2.4 Å resolution, Nat. Struct. Biol. 7 (2000) 1055–1061.
[74] V.K. Rastogi, M.E. Girvin, Structural changes linked to proton translocation by subunit *c* of the ATP synthase, Nature 402 (1999) 263–268.
[75] W.L. DeLano, The PyMOL Molecular Graphics System, DeLano Scientific, San Carlos, CA, USA, 2002.